JCTC Journal of Chemical Theory and Computation

Article

pubs.acs.org/JCTC

Solvated Charge Transfer States of Functionalized Anthracene and Tetracyanoethylene Dimers: A Computational Study Based on a Range Separated Hybrid Functional and Charge Constrained Self-Consistent Field with Switching Gaussian Polarized Continuum Models

Shaohui Zheng,*,† Eitan Geva,*,† and Barry D. Dunietz*,‡

†Department of Chemistry, University of Michigan, Ann Arbor, Michigan 48109, United States

‡Department of Chemistry, Kent State University, Kent, Ohio 44242, United States

Supporting Information

ABSTRACT: We benchmark several protocols for evaluating the energies of excited charge transfer (CT) states of organic molecules dissolved in polar liquids. The protocols combine time-dependent density functional theory using range-separated hybrid functionals, constrained density functional theory, dispersion corrected functional, and a dielectric continuum model for representing the solvent. We compare the different protocols against well-established experimental measured charge transfer state energies in solvated dimers of functionalized anthracene and tetracyanoethylene. We find that using the range-separated hybrid functional for the charge-transfer state energies and the combination of constrained density functional theory with the recently improved switching Gaussian polarizable continuum model (PCM) provide good agreement with the experimental values of the solvated CT states. We also find that using dispersion corrected solvated geometries for the weakly coupled donor−acceptor dimers considered here leads to improved agreement with experimental measured values.

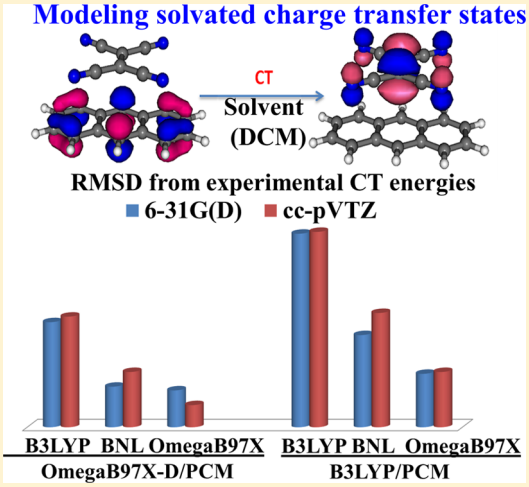

INTRODUCTION

Solvation by a polar medium can considerably stabilize charge-separated states.[1−6] However, accurately calculating the energies of charge transfer (CT) states of organic molecules interacting with a polar medium via density functional theory (DFT) is challenging for the following reasons: (1) There is a well-known tendency of conventional DFT to underestimate the energies of CT states.[7−9] (2) The polar medium affects the electronic structure of the CT states and thereby their geometries, transition frequencies, and transition dipole moments.[10−15]

One popular way for addressing the first challenge is by employing the recently developed long-range corrected (LRC) or range separated hybrid (RSH) functionals in linear response (LR) time-dependent (TD) DFT.[7,8,16−18] Another recent developed approach to treat CT states is based on constrained variational DFT (CV-DFT) including fourth order response terms.[19] These approaches have repeatedly been shown to reproduce accurate *gas-phase* electronic excited CT state energies.[16,17,20−31]

The second challenge is exacerbated in the case of spatially separated donor−acceptor (D−A) complexes, where the strong dipole moment associated with the CT leads to strong solvation effects in a polar medium.[14] The effect of solvation on localized excitations is addressed quite effectively by applying the LR formalism within the polarizable continuum model (PCM).[13−15,32−34] In the case of long-range CT states in solution, however, the LR scheme within PCM/TD-DFT tends to overestimate the shift in CT energy due to solvation.[35] In other words, the large extent of charge reorganization needs to be addressed when describing the excited states. In such cases, the excited electronic density has to be optimized as implemented, for example by the state specific (SS) PCM/TDDFT approach. However, SS-PCM/TDDFT applicability remains quite limited due to the complexity in the self-consistent optimization procedure.[14,35−38]

Alternatively, the solvent effect on a CT state can be addressed using charge constrained DFT (C-DFT)[13−15,32−34,39−41] combined with dielectric continuum models, such as PCM.[13,24,42] We previously used such an approach to explain the enhanced red-shift between emission and absorption of chromophores that functionalize silsesquiox-

Received: May 29, 2012
Published: January 22, 2013

anes.[1] The observed red-shifting of the spectra is explained as originating from charge transfer between chromophores.

In the present paper, we consider several modifications to the original protocol used in ref 1. The variations mainly pertain to the geometry optimization. We test the new protocols systematically against an experimental measured benchmark set of solvated CT states. The set consists of D−A dimers of functionalized anthracenes (X−AR, X = 9nitro-, 9formyl,10Cl-, 9Cl-, 9,10Br-, 9Br-, 9acetyl-, 9phenyl-, 9,10dimethyl-, 9methyl-, and 2methyl-) and tetracyanoethylene (TCNE) dissolved in methylene chloride (CH_2Cl_2).[43] In these dimers, TCNE serves as the electron acceptor, and the functionalized X−AR as the donor of the photoexcited electron. We find that all the CT states in the dimer set correspond to a complete electron transfer between the HOMO on X−AR and the LUMO on the TCNE. We illustrate, for example, the HOMO and LUMO electron densities associated with the excited CT state of the unfunctionalized dimer in Figure 1. Extrapolated gas phase CT

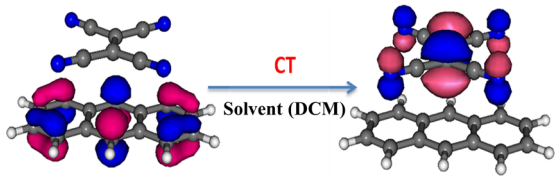

Figure 1. The HOMO (left) and LUMO (right) electron densities involved with charge transfer in the anthracene−TCNE dimer.

state energies of this series have been recently used[19,23] to demonstrate the accuracy of the RSH Baer−Neuhauser−Livshits (BNL) functional[23] and the CV-DFT approach.[19] In the present paper, we extend the analysis to account for the energies of the *solvated* CT excited states. More specifically, we show that good agreement with experimental results can be achieved by combining the following elements: (1) obtaining the gas-phase CT state energies using TDDFT with the BNL functional, (2) obtaining the ground state solvated geometries using DFT with the OmegaB97X-D dispersion corrected functional and the recently implemented switching Gaussian PCM model for the solvent effects, and (3) obtaining solvation energies using C-DFT with PCM.

COMPUTATIONAL DETAILS

In the first step of our protocol, we calculate the *gas-phase* excited CT state energies via TDDFT and for completeness also the Tamm−Dancoff approximation[1,44−46] (TDA). The performance of the following density functionals was compared: (1) B3LYP,[47,48] (2) BNL,[23,49,50] and (3) OmegaB97X.[29] For geometry optimizations, we compare between using the B3LYP functional and a dispersion corrected functional, the OmegaB97X-D functional.[28]

The BNL functional involves a system-specific parameter, γ, which is evaluated by minimizing the following function:[23,49,50]

$$J(\gamma) = |\varepsilon_{\mathrm{HOMO}}(N;\gamma) + \mathrm{IP}(N;\gamma)|^2 + |\varepsilon_{\mathrm{HOMO}}(N+1;\gamma) + \mathrm{IP}(N+1;\gamma)|^2 \quad (1)$$

Here

$$\mathrm{IP}(N;\gamma) = E(N-1;\gamma) - E(N;\gamma) \quad (2)$$

where IP is the ionization potential of the system, N or $N+1$ is the number of electrons in the system, and $\varepsilon_{\mathrm{HOMO}}$ is the energy of the HOMO Kohn−Sham orbital.

We calculate the solvation energies that shift the gas phase CT energies:

$$E^{\mathrm{TDDFT}}_{\mathrm{Solvated}} = E^{\mathrm{TDDFT}}_{\mathrm{Gas}} + E^{\mathrm{CT}}_{\mathrm{Solvation}} \quad (3)$$

The solvation energy is evaluated using a modern implementation of the PCM based on switching/Gaussians (SWIG) for smooth electronic densities[42] as follows:

$$E^{\mathrm{CT}}_{\mathrm{Solvation}} = [E^{\mathrm{CT}}(\mathrm{PCM}) - E(\mathrm{PCM}, \mathrm{Ground})] - [E^{\mathrm{CT}}(\mathrm{Gas}) - E(\mathrm{Gas}, \mathrm{Ground})] \quad (4)$$

Here, E^{CT}(PCM/Gas) and E(PCM/Gas, Ground) denote the CT and ground energies with/without the dielectric continuum, respectively. In calculating the solvation energy in eq 4, the CT state energies are evaluated via C-DFT.[39−41]

The C-DFT is essentially a ground state DFT description with imposed constraints to satisfy designated atomic charges within the self-consistent optimization of the electronic density. The constraints ($W[\rho]$) applied to the electronic density (ρ) are based on a spatial weight function (w), which imposes the chosen charge distribution:

$$\mathrm{W}[\rho] = \int w(r)\,\rho(r)\,\mathrm{d}^3r - N \quad (5)$$

Here, N is the target electron number defining the charge constraint. The spatial weight function w is used to designate charged regions in the system as the donor and acceptor sites. The imposed constraint on the spatial charge distribution is based on atomic charge populations. For example, it can be set to (−1) charge on the acceptor site atoms and (+1) on the designated donor atoms. The constraint is added to the density functional, $E[\rho]$, where V is a Lagrange multiplier related to the charging constraint:

$$E'[\rho, V] = E[\rho] + VW[\rho] \quad (6)$$

Clearly, an important detail in the implementation of C-DFT calculations is the scheme by which the weighting function is evaluated. We follow the recent applications of C-DFT,[39,51] where the B3LYP functional is employed to obtain the lowest gas-phase and PCM-solvated CT state energies.[39−41,51,52] The atomic charges are determined by the Becke charge population scheme.[40,51] The Becke scheme has been proved to provide a more consistent performance for C-DFT calculations than alternative implementations using Mulliken or Lowdin atomic-orbital-based analysis of the charge population.[52]

For the weakly coupled acceptor−donor sites, the CT states are expected to involve a (close to) whole electron transfer. Indeed, we confirm that in the dimer systems we analyze below that the TDDFT CT excited states correspond to +1/−1 Mulliken charge. We also point out that the CDFT calculations that generate the +1/−1 Mulliken charges are obtained by imposing over ±0.9 Becke charges in the donor and acceptor regions.

In all calculations, we expand the electronic density in the cc-pVTZ atomic basis set based on the geometries obtained from omgegaB97X-D or B3LYP PCM/6-31G(D) levels. We confirm that smaller basis sets (6-31G(D)) generate similar excitation energies within 0.3 eV and a similar root-mean-square deviation (RMSD) from experimental results. All calculations were

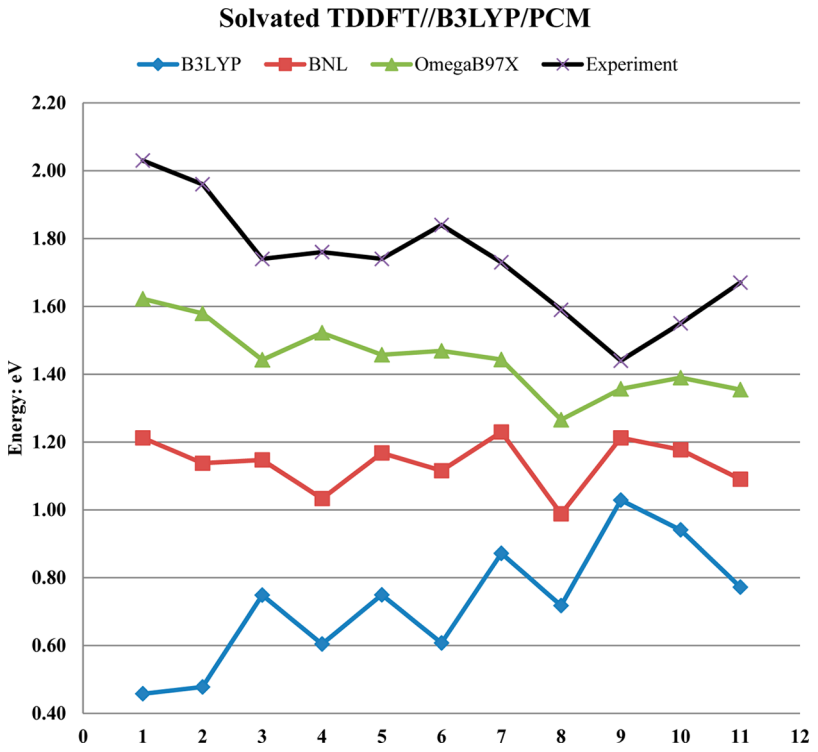

Figure 2. The solvated TDDFT CT state energies at the B3LYP/PCM optimized ground state geometry and the experimental values (see SI, Table S1 for numerical values). Number and substitution: (1) 9nitro-, (2) 9formyl,10Cl-, (3) 9Cl-, (4) 9,10Br-, (5) 9Br-, (6) 9acetyl-, (7) None, (8) 9phenyl-, (9) 9,10dimethyl-, (10) 9methyl-, (11) 2methyl-.

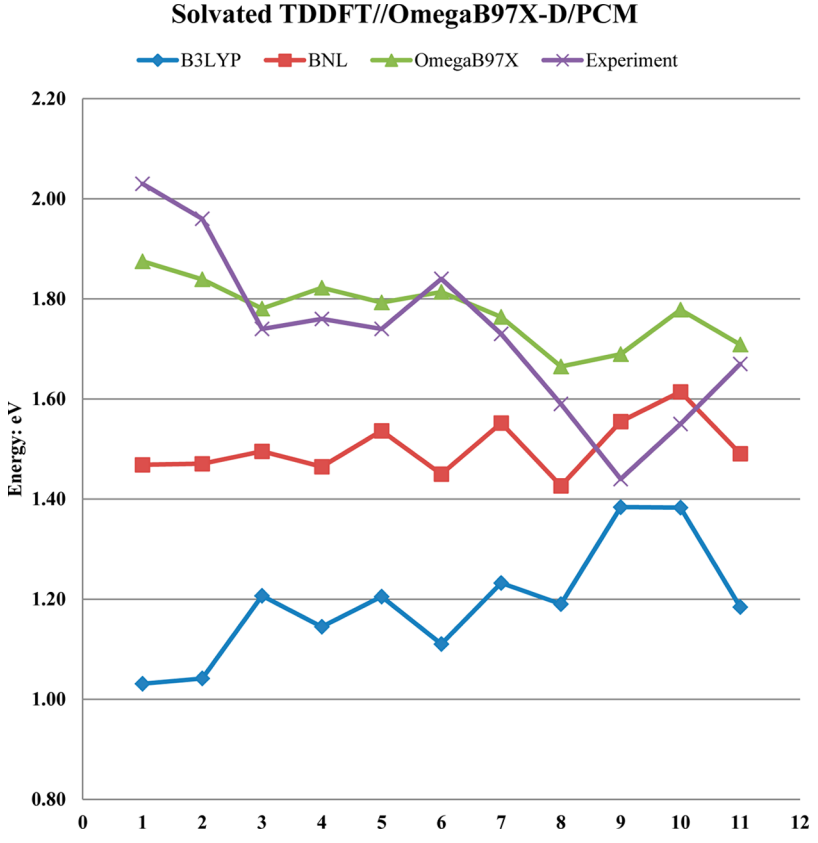

Figure 3. The solvated TDDFT CT state energies at the OmegaB97X-D/PCM optimized ground state geometry and the experimental values (see SI Table S2 for numerical values). The correspondence between the molecule number and the substitution is provided in Figure 2.

dx.doi.org/10.1021/ct300700q | J. Chem. Theory Comput. 2013, 9, 1125−1131

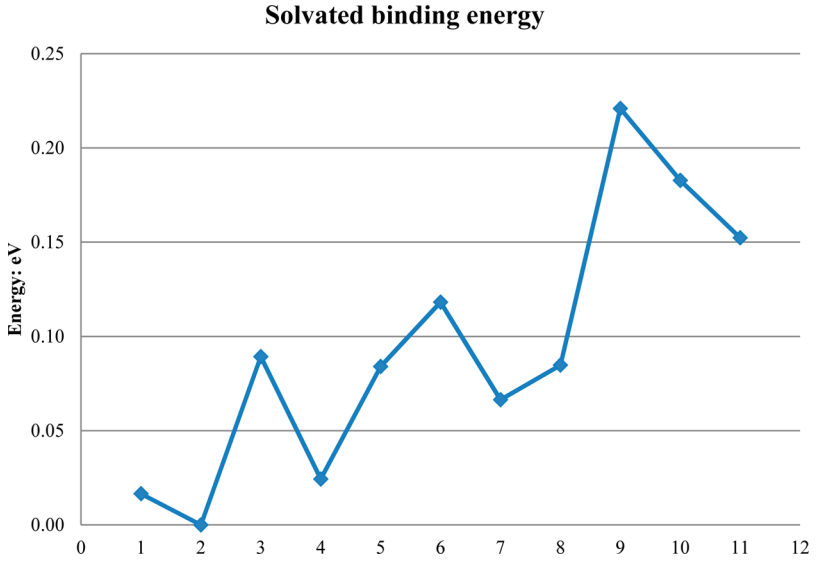

Figure 4. The solvated binding energies of the TCNE-AR series at OmegaB97X-D/PCM optimized geometries.

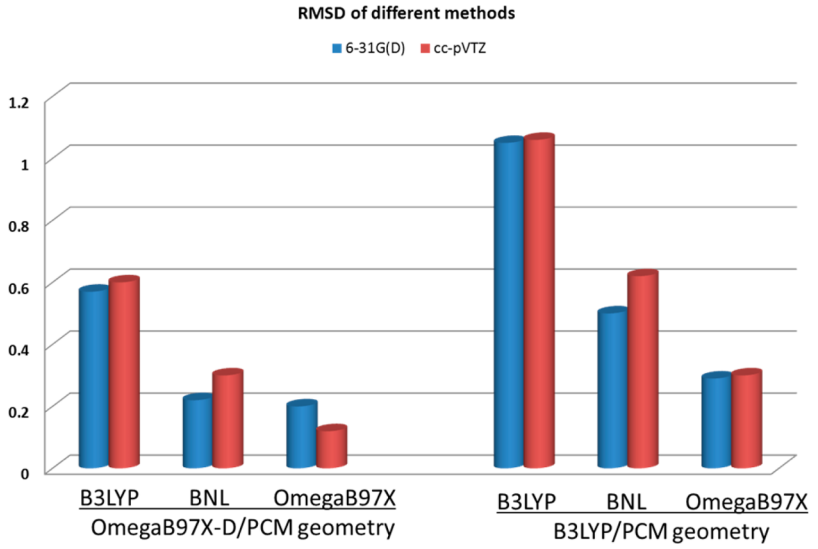

Figure 5. RMSDs between calculated and experimental energies (eV) for different methods and geometries: TDDFT using the B3LYP, BNL, and OmegaB97X functionals with cc-pVTZ and 6-31G(D) basis sets at the B3LYP/PCM and OmegaB97X-D/PCM optimized geometries.

implemented using Q-CHEM prerelease package version 4.0.[53,54]

RESULTS AND DISCUSSIONS

We have ordered the molecules by increasing electron donating character of their substitution group to identify trends affecting the calculated solvation energies. We compare the calculated CT energies among using TDDFT with B3LYP, BNL ,and OmegaB97X functionals. We start by using optimized solvated ground state geometries at the B3LYP/6-31G(D)/PCM level (see data in Figure 2). The corresponding energies are listed in SI Table S1, where we also provide the gas phase energies. We find that the solvated CT state energies obtained via B3LYP significantly underestimate the corresponding experimental values. The B3LYP results underestimate the energies by 1.1 eV for the root-mean-square deviation (RMSD) from the experimental values, while BNL and OmegaB97X underestimate the corresponding experimental values by 0.6 and 0.3 eV for the RMSD, respectively.

We next consider the solvation energies using dispersion-corrected geometries at the OmegaB97X-D/6-31G(D)/PCM level (see data in Figure 3 and listing in SI Table S2). In a recent study, the importance of van der Waals interactions in determining CT state energies and geometries has been demonstrated on several gas phase D−A dimer models.[55] The CT state energies calculated at the dispersion corrected ground state geometries are in better agreement with the measured values for all the functionals considered. However, B3LYP still considerably underestimates the solvated CT energies for molecules 1−8 and 11. We find that the RSH functionals slightly overestimate the energies for molecules 9 and 10. We also note that the BNL excited state energies are lower than the OmegaB97X, providing a consistent underestimation of the energy that is decreasing with the molecule number (electron donating effect). The solvation energies and D−A separation distances for both series (B3LYP and OmegaB97X-D based geometries) are well converged (the values are listed in SI Table S3 and compared to the 6-31G(d)

dx.doi.org/10.1021/ct300700q | J. Chem. Theory Comput. 2013, 9, 1125−1131

basis set in SI Table S4). We supplement these results by comparing the TDDFT gas phase in both basis sets with the TDA based results. The TDDFT energies are in agreement within 0.3 eV for the B3LYP/PCM based geometries (see SI Tables S5 and S6).

We next correlate the deviation from experimental values with the dimer binding energies. We define the dimer binding energy simply as the difference between the dimer energy in PCM, E(Dimer, PCM), and the sum of the monomer energies in PCM, E(D/A, PCM):

$$E_{\text{Binding}} = E(\text{D, PCM}) + E(\text{A, PCM}) - E(\text{dimer, PCM}) \quad (7)$$

The binding energies of the different dimers in solution at the B3LYP/cc-pVTZ/PCM level are provided in Figure 4 with the values listed in SI Table S7. The basis set superposition error (BSSE) of the gas phase binding energy is found to be smaller than 0.04 eV for all dimers. As expected, the binding energy increases with decreasing strength of the electron withdrawing groups (EWG). More specifically, molecules 1 and 2, with the strongest EWG, have the weakest dimer binding energies, whereas molecules 9 and 10, with the strongest electron donating groups (EDG), have the strongest binding energies.

We therefore hypothesize that the donor−acceptor separation of molecules 9 and 10 is underestimated in our models in comparison to the actual systems and therefore leads to underestimating the solvation energy. Our models capture weak intermolecular attractive forces that most likely are broken by explicit solvent molecules and thermal fluctuations. The situation is quite different for dimers 1 and 2 with the strongest EWG substitutions including the formyl and nitro groups.[56] In these cases, using OmegaB97X-D in the geometry optimizations appears to overestimate the strong electrostatic repulsive interactions, thereby overestimating the donor−acceptor separation leading to overestimating the solvation energy. The overestimated electrostatic interactions result from the limited ability to account for screening within PCM.

CONCLUSIONS

Finally, we provide the calculated solvation energy RMSD from the experimental values for the different schemes in Figure 5. We find that both the BNL and the OmegaB97X based protocols outperform the B3LYP functional based approach for calculating the CT states energies. The two functionals demonstrate overall similar results when using the dispersion corrected geometries. The OmegaB97X with no tunable parameter is, therefore, a good alternative to the BNL functional, which requires reoptimization of a range separation parameter. Interestingly, however, the OmegaB97X features quite limited sensitivity to the geometry, whereas the BNL functional seems more reliable with greater sensitivity of the CT energetics to geometry variations. We also find that the smaller basis set 6-31G(D) has similar performance to the cc-pVTZ basis set.

In summary, using a protocol that combines RSH-TDDFT and C-DFT/PCM, we are able to reproduce, rather accurately, the solvated CT state energies in the AR-TCNE dimer series. The protocol described in this work is therefore shown to be an efficient alternative to a full implementation of TDDFT with PCM. The importance of using correct solvated dimer geometries for obtaining the reliable CT state energies was also demonstrated. This is especially true for weakly coupled CT systems in solution and in particular for the π-stacked systems considered in this work. Indeed, we find that the overall agreement with experimental results is improved by using dispersion-corrected dimer geometries.

ASSOCIATED CONTENT

Supporting Information

Supporting Information of CT states energies as referred to is provided in the form of tables. This material is available free of charge via the Internet at http://pubs.acs.org.

AUTHOR INFORMATION

Corresponding Author

*E-mail: jjkzhg@gmail.com; eitan@umich.edu; bdunietz@kent.edu.

Notes

The authors declare no competing financial interest.

ACKNOWLEDGMENTS

B.D.D. and E.G. acknowledge the U.S. Department of Energy Office of Science, Office of Basic Energy Sciences for funding. This work is pursued as part of the Center for Solar and Thermal Energy Conversion, an Energy Frontier Research Center under Award No. DE-SC0000957. S.Z. thanks Heidi Philips for her help to create this manuscript and David Braun for computing support.

REFERENCES

(1) Zheng, S.; Phillips, H.; Geva, E.; Dunietz, B. D. Ab Initio Study of the Emissive Charge-Transfer States of Solvated Chromophore-Functionalized Silsesquioxanes. *J. Am. Chem. Soc.* **2012**, *134*, 6944−6947.

(2) Ogunsipe, A.; Maree, D.; Nyokong, T. Solvent effects on the photochemical and fluorescence properties of zinc phthalocyanine derivatives. *J. Mol. Struct.* **2003**, *650*, 131−140.

(3) Sulaiman, S.; Bhaskar, A.; Zhang, J.; Guda, R.; Goodson, T.; Laine, R. M. Molecules with perfect cubic symmetry as nanobuilding blocks for 3-D assemblies. Elaboration of octavinylsilsesquioxane. Unusual luminescence shifts may indicate extended conjugation involving the silsesquioxane core. *Chem. Mater.* **2008**, *20*, 5563−5573.

(4) Barthel, E. R.; Martini, I. B.; Schwartz, B. J. How does the solvent control electron transfer? Experimental and theoretical studies of the simplest charge transfer reaction. *J. Phys. Chem. B* **2001**, *105*, 12230−12241.

(5) El-Khouly, M. E.; Ito, O.; Smith, P. M.; D'Souza, F. Intermolecular and supramolecular photoinduced electron transfer processes of fullerene-porphyrin/phthalocyanine systems. *J. Photochem. Photobiol., C* **2004**, *5*, 79−104.

(6) Laenen, R.; Roth, T.; Laubereau, A. Novel precursors of solvated electrons in water: Evidence for a charge transfer process. *Phys. Rev. Lett.* **2000**, *85*, 50−53.

(7) Dreuw, A.; Head-Gordon, M. Single-reference ab initio methods for the calculation of excited states of large molecules. *Chem. Rev.* **2005**, *105*, 4009−4037.

(8) Dreuw, A.; Head-Gordon, M. Failure of time-dependent density functional theory for long-range charge-transfer excited states: The zincbacteriochlorin-bacterlochlorin and bacteriochlorophyll-spheroidene complexes. *J. Am. Chem. Soc.* **2004**, *126*, 4007−4016.

(9) Dreuw, A.; Weisman, J. L.; Head-Gordon, M. Long-range charge-transfer excited states in time-dependent density functional theory require non-local exchange. *J. Chem. Phys.* **2003**, *119*, 2943−2946.

(10) Govind, N.; Valiev, M.; Jensen, L.; Kowalski, K. Excitation Energies of Zinc Porphyrin in Aqueous Solution Using Long-Range Corrected Time-Dependent Density Functional Theory. *J. Phys. Chem. A* **2009**, *113*, 6041−6043.

(11) Autschbach, J.; Zheng, S. H. Density functional computations of Ru-99 chemical shifts: Relativistic effects, influence of the density functional, and study of solvent effects on fac- Ru(CO)(3)I-3 (-). *Magn. Reson. Chem.* **2006**, *44*, 989−1007.
(12) Zheng, S.; Autschbach, J. Modeling of Heavy-Atom−Ligand NMR Spin−Spin Coupling in Solution: Molecular Dynamics Study and Natural Bond Orbital Analysis of Hg-C Coupling Constants. *Chem.—Eur. J.* **2011**, *17*, 161−173.
(13) Cances, E.; Mennucci, B.; Tomasi, J. A new integral equation formalism for the polarizable continuum model: Theoretical background and applications to isotropic and anisotropic dielectrics. *J. Chem. Phys.* **1997**, *107*, 3032−3041.
(14) Mennucci, B.; Cappelli, C.; Guido, C. A.; Camlmi, R.; Tomasi, J. Structures and Properties of Electronically Excited Chromophores in Solution from the Polarizable Continuum Model Coupled to the Time-Dependent Density Functional Theory. *J. Phys. Chem. A* **2009**, *113*, 3009−3020.
(15) Mennucci, B.; Tomasi, J. Continuum solvation models: A new approach to the problem of solute's charge distribution and cavity boundaries. *J. Chem. Phys.* **1997**, *106* (12), 5151−5158.
(16) Baer, R.; Livshits, E.; Salzner, U. Tuned Range-Separated Hybrids in Density Functional Theory. *Annu. Rev. Phys. Chem.* **2010**, *61*, 85−109.
(17) Baer, R.; Neuhauser, D. Density functional theory with correct long-range asymptotic behavior. *Phys. Rev. Lett.* **2005**, *94*, 043002.
(18) Livshits, E.; Baer, R. A well-tempered density functional theory of electrons in molecules. *Phys. Chem. Chem. Phys.* **2007**, *9*, 2932−2941.
(19) Ziegler, T.; Krykunov, M. On the calculation of charge transfer transitions with standard density functionals using constrained variational density functional theory. *J. Chem. Phys.* **2010**, *133*, 074104.
(20) Andzelm, J.; Rinderspacher, B. C.; Rawlett, A.; Dougherty, J.; Baer, R.; Govind, N. Performance of DFT Methods in the Calculation of Optical Spectra of TCF-Chromophores. *J. Chem. Theory Comput.* **2009**, *5*, 2835−2846.
(21) Srebro, M.; Autschbach, J. Tuned Range-Separated Time-Dependent Density Functional Theory Applied to Optical Rotation. *J. Chem. Theory Comput.* **2012**, *8* (1), 245−256.
(22) Livshits, E.; Baer, R. Time-dependent density-functional studies of the D-2 Coulomb explosion. *J. Phys. Chem. A* **2006**, *110*, 8443−8450.
(23) Stein, T.; Kronik, L.; Baer, R. Reliable Prediction of Charge Transfer Excitations in Molecular Complexes Using Time-Dependent Density Functional Theory. *J. Am. Chem. Soc.* **2009**, *131* (8), 2818−2820.
(24) Lange, A.; Herbert, J. M. Simple methods to reduce charge-transfer contamination in time-dependent density-functional calculations of clusters and liquids. *J. Chem. Theory Comput.* **2007**, *3*, 1680−1690.
(25) Rohrdanz, M. A.; Martins, K. M.; Herbert, J. M. A long-range-corrected density functional that performs well for both ground-state properties and time-dependent density functional theory excitation energies, including charge-transfer excited states. *J. Chem. Phys.* **2009**, *130* (5), 054112.
(26) Jacquemin, D.; Perpete, E. A.; Scuseria, G. E.; Ciofini, I.; Adamo, C. TD-DFT performance for the visible absorption spectra of organic dyes: Conventional versus long-range hybrids. *J. Chem. Theory Comput.* **2008**, *4*, 123−135.
(27) Yanai, T.; Tew, D. P.; Handy, N. C. A new hybrid exchange-correlation functional using the Coulomb-attenuating method (CAM-B3LYP). *Chem. Phys. Lett.* **2004**, *393*, 51−57.
(28) Chai, J. D.; Head-Gordon, M. Long-range corrected hybrid density functionals with damped atom-atom dispersion corrections. *Phys. Chem. Chem. Phys.* **2008**, *10* (44), 6615−6620.
(29) Chai, J. D.; Head-Gordon, M. Systematic optimization of long-range corrected hybrid density functionals. *J. Chem. Phys.* **2008**, *128*, 084106.
(30) Autschbach, J. Charge-Transfer Excitations and Time-Dependent Density Functional Theory: Problems and Some Proposed Solutions. *ChemPhysChem* **2009**, *10*, 1757−1760.
(31) Sini, G.; Sears, J. S.; Bredas, J. L. Evaluating the Performance of DFT Functionals in Assessing the Interaction Energy and Ground-State Charge Transfer of Donor/Acceptor Complexes: Tetrathiafulvalene-Tetracyanoquinodimethane (TTF-TCNQ) as a Model Case. *J. Chem. Theory Comput.* **2011**, *7*, 602−609.
(32) Gustavsson, T.; Banyasz, A.; Lazzarotto, E.; Markovitsi, D.; Scalmani, G.; Frisch, M. J.; Barone, V.; Improta, R. Singlet excited-state behavior of uracil and thymine in aqueous solution: A combined experimental and computational study of 11 uracil derivatives. *J. Am. Chem. Soc.* **2006**, *128*, 607−619.
(33) Improta, R.; Scalmani, G.; Frisch, M. J.; Barone, V. Toward effective and reliable fluorescence energies in solution by a new state specific polarizable continuum model time dependent density functional theory approach. *J. Chem. Phys.* **2007**, *127*, 074504.
(34) Santoro, F.; Improta, R.; Lami, A.; Bloino, J.; Barone, V. Effective method to compute Franck-Condon integrals for optical spectra of large molecules in solution. *J. Chem. Phys.* **2007**, *126* (8), 084509.
(35) Mennucci, B. Polarizable continuum model. *Wiley Interdiscip. Rev.: Comput. Mol. Sci.* **2012**, *2*, 386−404.
(36) Caricato, M.; Mennucci, B.; Scalmani, G.; Trucks, G. W.; Frisch, M. J. Electronic excitation energies in solution at equation of motion CCSD level within a state specific polarizable continuum model approach. *J. Chem. Phys.* **2010**, *132*, 084102.
(37) Marenich, A. V.; Cramer, C. J.; Truhlar, D. G.; Guido, C. A.; Mennucci, B.; Scalmani, G.; Frisch, M. J. Practical computation of electronic excitation in solution: vertical excitation model. *Chem. Sci.* **2011**, *2*, 2143−2161.
(38) Improta, R. The excited states of pi-stacked 9-methyladenine oligomers: a TD-DFT study in aqueous solution. *Phys. Chem. Chem. Phys.* **2008**, *10*, 2656−2664.
(39) Van Voorhis, T.; Kowalczyk, T.; Kaduk, B.; Wang, L. P.; Cheng, C. L.; Wu, Q. The Diabatic Picture of Electron Transfer, Reaction Barriers, and Molecular Dynamics. *Annu. Rev. Phys. Chem.* **2010**, *61*, 149−170.
(40) Wu, Q.; Van Voorhis, T. Constrained density functional theory and its application in long-range electron transfer. *J. Chem. Theory Comput.* **2006**, *2*, 765−774.
(41) Wu, Q.; Van Voorhis, T. Direct calculation of electron transfer parameters through constrained density functional theory. *J. Phys. Chem. A* **2006**, *110*, 9212−9218.
(42) Jacobson, L. D.; Herbert, J. M. Polarization-Bound Quasi-Continuum States Are Responsible for the "Blue Tail" in the Optical Absorption Spectrum of the Aqueous Electron. *J. Am. Chem. Soc.* **2010**, *132*, 10000−10002.
(43) Masnovi, J. M.; Seddon, E. A.; Kochi, J. K. Electron-transfer from anthracenes - comparison of photoionization, charge-transfer excitation and electrochemical oxidation. *Can. J. Chem.* **1984**, *62*, 2552−2559.
(44) Hirata, S.; Head-Gordon, M. Time-dependent density functional theory within the Tamm-Dancoff approximation. *Chem. Phys. Lett.* **1999**, *314*, 291−299.
(45) Phillips, H.; Zheng, S.; Hyla, A.; Laine, R.; Goodson, T.; Geva, E.; Dunietz, B. D. Ab Initio Calculation of the Electronic Absorption of Functionalized Octahedral Silsesquioxanes via Time-Dependent Density Functional Theory with Range-Separated Hybrid Functionals. *J. Phys. Chem. A* **2012**, *116*, 1137−1145.
(46) Hsu, C. P.; Hirata, S.; Head-Gordon, M. Excitation energies from time-dependent density functional theory for linear polyene oligomers: Butadiene to decapentaene. *J. Phys. Chem. A* **2001**, *105*, 451−458.
(47) Lee, C.; Yang, W.; Parr, R. G. Development of the Colle-Salvetti correlation-energy formula into a functional of the electron density. *Phys. Rev. B* **1988**, *37*, 785−789.
(48) Stephens, P. J.; Devlin, F. J.; Chabalowski, C. F.; Frisch, M. J. Ab-initio calculation of vibrational absorption and circular-dichroism

spectra using density-functional force-fields. *J. Phys. Chem.* **1994**, *98*, 11623−11627.
(49) Stein, T.; Kronik, L.; Baer, R. Prediction of charge-transfer excitations in coumarin-based dyes using a range-separated functional tuned from first principles. *J. Chem. Phys.* **2009**, *131*, 244119.
(50) Kuritz, N.; Stein, T.; Baer, R.; Kronik, L. Charge-Transfer-Like pi(->)pi* Excitations in Time-Dependent Density Functional Theory: A Conundrum and Its Solution. *J. Chem. Theory Comput.* **2011**, *7*, 2408−2415.
(51) Wu, Q.; Van Voorhis, T. Direct optimization method to study constrained systems within density-functional theory. *Phys. Rev. A* **2005**, *72*, 024502.
(52) Kaduk, B.; Kowalczyk, T.; Van Voorhis, T. Constrained Density Functional Theory. *Chem. Rev.* **2012**, *112*, 321−370.
(53) Kong, J.; White, C. A.; Krylov, A. I.; Sherrill, D.; Adamson, R. D.; Furlani, T. R.; Lee, M. S.; Lee, A. M.; Gwaltney, S. R.; Adams, T. R.; Ochsenfeld, C.; Gilbert, A. T. B.; Kedziora, G. S.; Rassolov, V. A.; Maurice, D. R.; Nair, N.; Shao, Y. H.; Besley, N. A.; Maslen, P. E.; Dombroski, J. P.; Daschel, H.; Zhang, W. M.; Korambath, P. P.; Baker, J.; Byrd, E. F. C.; Van Voorhis, T.; Oumi, M.; Hirata, S.; Hsu, C. P.; Ishikawa, N.; Florian, J.; Warshel, A.; Johnson, B. G.; Gill, P. M. W.; Head-Gordon, M.; Pople, J. A. Q-chem 2.0: A high-performance ab initio electronic structure program package. *J. Comput. Chem.* **2000**, *21*, 1532−1548.
(54) Shao, Y.; Molnar, L. F.; Jung, Y.; Kussmann, J.; Ochsenfeld, C.; Brown, S. T.; Gilbert, A. T. B.; Slipchenko, L. V.; Levchenko, S. V.; O'Neill, D. P.; DiStasio, R. A.; Lochan, R. C.; Wang, T.; Beran, G. J. O.; Besley, N. A.; Herbert, J. M.; Lin, C. Y.; Van Voorhis, T.; Chien, S. H.; Sodt, A.; Steele, R. P.; Rassolov, V. A.; Maslen, P. E.; Korambath, P. P.; Adamson, R. D.; Austin, B.; Baker, J.; Byrd, E. F. C.; Dachsel, H.; Doerksen, R. J.; Dreuw, A.; Dunietz, B. D.; Dutoi, A. D.; Furlani, T. R.; Gwaltney, S. R.; Heyden, A.; Hirata, S.; Hsu, C. P.; Kedziora, G.; Khalliulin, R. Z.; Klunzinger, P.; Lee, A. M.; Lee, M. S.; Liang, W.; Lotan, I.; Nair, N.; Peters, B.; Proynov, E. I.; Pieniazek, P. A.; Rhee, Y. M.; Ritchie, J.; Rosta, E.; Sherrill, C. D.; Simmonett, A. C.; Subotnik, J. E.; Woodcock, H. L.; Zhang, W.; Bell, A. T.; Chakraborty, A. K.; Chipman, D. M.; Keil, F. J.; Warshel, A.; Hehre, W. J.; Schaefer, H. F.; Kong, J.; Krylov, A. I.; Gill, P. M. W.; Head-Gordon, M. Advances in methods and algorithms in a modern quantum chemistry program package. *Phys. Chem. Chem. Phys.* **2006**, *8*, 3172−3191.
(55) Steinmann, S. N.; Piemontesi, C.; Delachat, A.; Corminboeuf, C. Why are the Interaction Energies of Charge-Transfer Complexes Challenging for DFT? *J. Chem. Theory Comput.* **2012**, *8*, 1629−2640.
(56) Josa, D.; Otero, J. R.; Lago, E. M. C. A DFT study of substituent effects in corannulene dimers. *Phys. Chem. Chem. Phys.* **2011**, *13*, 21139−21145.